Cooperative dynamics in semiflexibile unentangled polymer fluids Cooperative dynamics in semiflexibile unentangled polymer fluids

DATASET *in* THE JOURNAL OF CHEMICAL PHYSICS · JULY 2003

Impact Factor: 2.95 · DOI: 10.1063/1.1606674

1 AUTHOR:

Marina Guenza
University of Oregon
89 PUBLICATIONS **908** CITATIONS

SEE PROFILE

Cooperative dynamics in semiflexibile unentangled polymer fluids

M. Guenza

Citation: J. Chem. Phys. **119**, 7568 (2003); doi: 10.1063/1.1606674
View online: http://dx.doi.org/10.1063/1.1606674
View Table of Contents: http://jcp.aip.org/resource/1/JCPSA6/v119/i14
Published by the American Institute of Physics.

Cooperative dynamics in semiflexibile unentangled polymer fluids

M. Guenza
Institute of Theoretical Science, Materials Science Institute and Department of Chemistry, University of Oregon, Eugene, Oregon 97403

(Received 2 May 2003; accepted 15 July 2003)

We present a generalized Langevin equation for the dynamics of semiflexible polymer chains of finite size in a dynamically heterogeneous fluid. Local and global dynamical properties, calculated in the framework of this approach, display anomalous behavior in agreement with experiments and computer simulations. The presence of heterogeneous dynamics induces non-Fickian center-of-mass diffusion and an anomalous slowdown of intramolecular modes of motion. Intermolecular interactions mostly perturb lowest-index modes, which correspond to polymer global dynamics. Internal polymer stiffness induces anomalies in the relaxation of highest-index modes, which characterize local dynamics and monomer diffusion. © *2003 American Institute of Physics.*
[DOI: 10.1063/1.1606674]

I. INTRODUCTION

The dynamics of unentangled polymer fluids is conventionally described by the Rouse model wherein single-chain motion is driven by intramolecular entropic restoring forces and segmental friction, while the surrounding fluid is described as a continuum that provides only a heat bath to the tagged particle. Consequently, each molecule is free to diffuse through a structurally and dynamically uniform liquid, and the single-chain center-of-mass mean-square displacement follows linear-in-time, Fickian diffusion at all times.[1]

The Rouse model agrees with data in the long-time regime, $t > \tau_{\text{Rouse}}$ (where τ_{Rouse} is the longest intramolecular relaxation time), in that it correctly predicts the scaling exponents of bulk viscosity and diffusion coefficient.[1] In the short-time regime, $t < \tau_{\text{Rouse}}$, the Rouse model disagrees with computer simulations and experiments,[2–6] where the single-molecule center-of-mass mean-square displacement displays a subdiffusive regime, $\Delta R^2(t) \propto t^{\nu}$, with $\nu \approx 0.75-0.9$.

Inconsistencies of the Rouse equation in the short-time regime are not limited to center-of-mass dynamics. Computer simulations and experiments of polyethylene melt dynamics show that the monomer mean-square displacement[2,4–6] displays a subdiffusive regime scaling in time as t^{ν}, with $\nu \approx 0.6$, making it a higher exponent than that of Rouse with $\nu = 0.5$. This suggests that not only chain connectivity, but also local semiflexibility,[7] influence the dynamics at small time scales. The static correlation of polymer normal modes presents a scaling in the mode index p of p^{-3}, which disagrees with the Rouse scaling of p^{-2}.[8,9] Finally, relaxation of the normal modes follows a mode-dependent stretched exponential decay.[2,3]

In a recent analysis of computer simulations of unentangled polymer melts, we observed that the onset of anomalous center-of-mass diffusion is related to the presence of interconverting regions of slow and fast dynamics in the fluid, the so-called *dynamical heterogeneities*.[10] This phenomenon is generally observed in dense fragile fluids close to their glass transition.[11,12] We argue that the occurrence of heterogeneous dynamics in polymer melts far from their glass transition is a consequence of the interplay between chain connectivity and intermolecular excluded volume interactions, which induces frustration in the fluid.

With the purpose of describing the dynamics of a tagged polymer chain in a dynamically heterogeneous matrix, we developed a new microscopic theoretical approach for the dynamics of a group of chains undergoing correlated motion.[13] In the short-time regime, a separation of time scales for the relaxation of fast- and slow-rearranging domains is observed, and projector operator techniques apply.[14] We defined as slow relevant variables the space coordinates and momenta of monomers belonging to polymers undergoing slow cooperative dynamics. The surrounding region of molecules undergoing fast dynamics serves as a heat bath providing random forces and an effective friction coefficient, in the spirit of the conventional generalized Langevin equation (GLE) description of fluid dynamics.[14]

In this paper, we implement our original many-chain approach[13] to describe the cooperative dynamics of a group of *finite-size semiflexible* polymers. With this key development, the theory can be compared quantitatively with experimental and computational data. We then investigate by model calculations the effect of the interplay between intermolecular cooperative dynamics and intramolecular semiflexibility on the intramolecular single-chain dynamics. The predictions of this model for global and local dynamical properties agree well with the dynamical anomalies observed in computer simulations and experimental data.[15,16]

The paper is structured in the following manner: In Sec. II, we present a brief overview of the dynamics of a flexible, infinitely long polymer chain in a dynamically heterogeneous environment. The dynamics of a finite-size semiflexible chain undergoing slow cooperative dynamics is developed in Sec. III. Normal modes dynamics and mean-square distances in the new formalism are derived in Secs. IV and V, respectively. In Sec. VI, we discuss the effect of the interplay between intramolecular semiflexibility and intermolecular co-

operativity on single-chain dynamics using model calculations. A brief discussion concludes the paper.

II. THEORETICAL BACKGROUND

The cooperative dynamics of polymer chains is described in our approach[13] by a set of n coupled generalized Langevin equations, where explicit intramolecular and intermolecular contributions are present in the propagator and in the memory functions. Each equation of motion describes the dynamics of monomer a contained in polymer i as

$$\zeta_0 \frac{d\mathbf{r}_a^i(t)}{dt} = k_s \frac{\partial^2 \mathbf{r}_a^i(t)}{\partial a^2} + \frac{1}{\beta} \frac{\partial}{\partial \mathbf{r}_a^i(t)} \ln\left(\prod_{k<j}^{n} g(\mathbf{r}^j(t), \mathbf{r}^k(t)) \right) - \sum_{b \neq a} \int d\tau \Gamma_{a,b}^i(t-\tau) \frac{d\mathbf{r}_b^i(\tau)}{d\tau} - \sum_{b} \sum_{j \neq i}^{n} \int d\tau \Gamma'^{j}_{a,b}(t-\tau) \frac{d\mathbf{r}_b^j(\tau)}{d\tau} + \mathbf{F}_a^i(t), \quad (1)$$

where $\beta^{-1} = k_B T$ is the thermal energy, $k_s = 3/\beta l^2$ is the entropic intramolecular spring constant, ζ_0 is the monomer friction coefficient, and $\mathbf{F}_a^i(t)$ is the random force.[14] The intramolecular correlation of random forces is $\Gamma_{a,b}^i(t) = \beta/3 \langle \mathbf{F}_a^i(0) \cdot \mathbf{F}_b^{Q(i)}(t) \rangle$, where $\mathbf{F}_b^{Q(i)}(t)$ is the projected random force acting on bead b of polymer i. The correlation of random forces acting on different polymer chains is given by $\Gamma'^{j}_{a,b}(t) = \beta/3 \langle \mathbf{F}_a^i(0) \cdot \mathbf{F}_b^{Q(j)}(t) \rangle$, which implicitly depends on the van Hove distribution function, $g(\mathbf{r}^i(t), \mathbf{r}^j(t))$.

The set of coupled equations is derived from the Liouville equation for the dynamics of the entire fluid by carrying out a projection onto space and momenta coordinates for a group of molecules undergoing slow cooperative dynamics. Since there is a separation of time scales of relaxation between regions of slow and fast dynamics,[10] the basic assumption of the projection operator technique is well justified in this case. In the final equation, the dynamics of fast molecules enters through random forces and the friction coefficient of slow molecules.

Equation (1) recovers the GLE for a pair of interacting particles when $n=2$ and the degree of polymerization $N=1$. Henceforth, it correctly describes a simple system whose dynamics is driven only by intermolecular interactions. Also, Eq. (1) recovers Rouse dynamics when the van Hove distribution function $g(r,t)=1$, and the intramolecular memory function is discarded. Assuming that $g(r,t)=1$ is consistent with an intermolecular mean-force potential that decays on a time scale much shorter than the single tagged-chain relaxation. This approximation, which is the basis of the Rouse approach, holds in general for polymers in dilute solutions of small-molecule solvents, or in the long-time regime of semidilute or concentrated polymer solutions and melts.[10]

In general, the mean-force potential is not negligible for a time scale shorter than τ_{Rouse} and length scale smaller than the polymer radius of gyration $R_g = \sqrt{N/6} l$, where l is the statistical segment length and N is the degree of polymerization.[10] In a recent paper, we derived an approximate analytical form of the potential $W(R,t)$ between the centers of mass for a pair of polymers, which allows us to solve the main equation by normal-mode analysis,

$$W(R,t) = -\ln g(R,t) \approx \frac{27\sqrt{2}}{4\pi\sqrt{\pi}} \frac{1}{\sqrt{N}\rho^*} [1 - 108(\pi\rho^*)^{-2} N^{-1}] \times e^{-3R^2(t)/(4R_g^2)}. \quad (2)$$

The potential $W(R,t)$ is Gaussian and finite at all interpolymer distances and has a range on the order of R_g, in agreement with the Gaussian-core model.[17] At full polymer-polymer overlap, $W(0)$ decreases with increasing reduced fluid density, $\rho^* = \rho l^3$, reflecting the transition from compressible to incompressible systems, where ρ is the monomer number density. It also decreases with increasing polymer molecular weight due to the increasing interpenetrability of polymer chains. Both effects are in qualitative agreement with the behavior observed in computer simulations of semidilute polymer solutions.[17]

Since $W(R,t)$ becomes infinitesimally small when the distance $R(t)$ exceeds a few R_g, our approach predicts that intermolecular effects, and the associated anomalous dynamics, are confined to a region in space characterized by a length scale comparable to the molecular radius of gyration. The number of interacting polymer chains inside this region is given by $n \approx \sqrt{N}\rho l^3$. If we assume a diffusive mechanism of relaxation, the average time scale of decay of the dynamical heterogeneities corresponds to $t \approx \tau_{\text{Rouse}}$.

A Gaussian-core potential for the interactions between two statistical segments on different polymer chains, at a distance r, can be derived following a procedure analogous to the one described above, namely

$$w(r,t) \approx \frac{3\sqrt{3}}{8\pi\sqrt{\pi}} (N/\rho^*) [1 - 108(\pi\rho^*)^{-2} N^{-1}] \times e^{-3/4(r(t)/d)^2}, \quad (3)$$

where d is the monomer hard-core length. Although approximated, this monomer–monomer effective potential reproduces well the short-range decay observed in computer simulations.[15]

From the expressions of the potential, we derive the forces in Eq. (1). Time dependence of forces enters through the intermolecular distance between the centers of mass, which changes with interdiffusion. The distance is approximated by its statistical average and calculated self-consistently from the solution of Eq. (1). This procedure produces an effective mean-force potential that agrees well with computer simulations.[15,16]

When the intermolecular potential is approximated by a time-dependent Gaussian function, Eq. (1) becomes

$$\zeta_0\frac{d\mathbf{r}_a^i(t)}{dt}=k_s\frac{\partial^2\mathbf{r}_a^i(t)}{\partial a^2}-(n-1)k_{\text{inter}}(t)\mathbf{r}_a^i(t)+\sum_{j\neq i}^{n}k_{\text{inter}}(t)\mathbf{R}_{\text{c.m.}}^j(t)-\sum_{b\neq a}\int d\tau\Gamma_{a,b}^i(t-\tau)\frac{d\mathbf{r}_b^i(\tau)}{d\tau}-\sum_{b}\sum_{j\neq i}^{n}\int d\tau\Gamma_{a,b}'^j(t-\tau)\frac{d\mathbf{r}_b^j(\tau)}{d\tau}+\mathbf{F}_a^i(t), \quad (4)$$

where $k_{\text{inter}}(t)[\mathbf{R}_{\text{c.m.}}^{(r)}-\mathbf{r}_a^{(t)}]$ is the time-dependent intermolecular force.

III. COOPERATIVE DYNAMICS OF SEMIFLEXIBLE POLYMER CHAINS OF FINITE SIZE

To investigate the dynamics of finite-size molecules, it is convenient to rewrite Eq. (4) in matrix notation as

$$\zeta_0\frac{d\mathbf{r}(t)}{dt}=-k_s\mathbf{A}_{\text{tot}}\mathbf{r}(t)-\int d\tau\boldsymbol{\Gamma}_{\text{tot}}(t-\tau)\frac{d\mathbf{r}(\tau)}{d\tau}+\mathbf{F}(t), \quad (5)$$

where $\mathbf{r}(t)=\mathbf{r}^{(1)}(t),\mathbf{r}^{(2)}(t),\ldots,\mathbf{r}^{(n)}(t)$ and $\mathbf{F}(t)=\mathbf{F}^{(1)}(t),\mathbf{F}^{(2)}(t),\ldots,\mathbf{F}^{(n)}(t)$ are column vectors of dimension $nN\times 1$. Each vector $\mathbf{r}(t)$ contains the coordinates of bead positions for N monomers belonging to n polymers comprised in the mean-force potential range. Random forces are represented by $\mathbf{F}(t)$. In the Markovian limit we define the effective friction coefficient as

$$\zeta_{\text{eff}}=\zeta_0+\frac{\beta}{3}\sum_{\alpha,\beta}^{nN}\int_0^\infty dt[\boldsymbol{\Gamma}_{\text{tot}}(t)]_{\alpha,\beta}. \quad (6)$$

The memory matrix $\boldsymbol{\Gamma}_{\text{tot}}(t)$ is a block matrix with n identical blocks on the diagonal given by the self-part of the memory contribution, the $N\times N$ $\boldsymbol{\Gamma}$ matrix, and $n(n-1)$ off-diagonal blocks that are given by the cross part of the memory term, the $N\times N$ $\boldsymbol{\Gamma}'$ matrix. We assume $\Gamma_{aa}=0$ because the self-correlation of random forces has already been taken into account as the bare friction coefficient ζ_0.

The $nN\times nN$ matrix $\mathbf{A}_{\text{tot}}$ is defined as

$$\mathbf{A}_{\text{tot}}=\mathbf{A}_{\text{intra}}+\frac{k_{\text{inter}}(t)}{k_s}\mathbf{A}_{\text{inter}}. \quad (7)$$

The matrix $\mathbf{A}_{\text{intra}}$ is a block diagonal matrix with n equivalent blocks on the diagonal identifying the n polymer chains. Each block is a $N\times N$ matrix $\mathbf{A}$, which contains information on the structure and interactions within a single polymer chain (intramolecular potential). For a flexible chain, the matrix $\mathbf{A}=\mathbf{A}_{\text{Rouse}}$, which is the Rouse matrix of nearest-neighbor force constants,[1] while for a semiflexible chain

$$\mathbf{A}=\frac{1-g}{1+g}\mathbf{A}_{\text{Rouse}}+\frac{g}{1-g}\mathbf{A}_{\text{Rouse}}^2-\frac{g^2}{1-g^2}\boldsymbol{\Delta}, \quad (8)$$

where $\boldsymbol{\Delta}$ is a local perturbation matrix important at high stiffness.[18] The first term in Eq. (8) simply describes a renormalized Gaussian freely jointed chain, where stiffness is incorporated by the effective Kuhn segment. The stiffness parameter $g=\langle\mathbf{l}_i\cdot\mathbf{l}_{i+1}\rangle\, l^{-2}$ is related to the polymer persistence length P through the relation $P/l\approx(1-g)^{-1}$.

The intermolecular contribution has a more complex form. The matrix $\mathbf{A}_{\text{inter}}$ is formed by $n\times n$ blocks of dimension $N\times N$, with n equivalent block matrices on the diagonal $\mathbf{A}_S$, and $n(n-1)$ identical off-diagonal block matrices $\mathbf{A}_U$. Now, $\mathbf{A}_S=(n-1)\mathbf{1}$, where $\mathbf{1}$ is the $N\times N$ identity matrix, while $(\mathbf{A}_U)_{i,j}=-1/N$ for any i and j. The total matrix $\mathbf{A}_{\text{tot}}$ is a block matrix with off-diagonal blocks equal to $\mathbf{A}_U$, and on-diagonal blocks equal to $\mathbf{A}_{\text{intra}}+\mathbf{A}_S$. The structure of the matrix $\mathbf{A}_{\text{tot}}$ can be simplified by performing a similarity transformation through the orthogonal matrix $\mathbf{T}$,

$$\mathbf{T}^T\mathbf{A}_{\text{tot}}\mathbf{T}=\begin{bmatrix}\mathbf{A}_D & \mathbf{0} & \cdots & \mathbf{0} & \mathbf{0}\\ \mathbf{0} & \mathbf{A}_D & \cdots & \mathbf{0} & \mathbf{0}\\ \cdots & \cdots & \cdots & \cdots & \cdots\\ \mathbf{0} & \mathbf{0} & \cdots & \mathbf{A}_D & \mathbf{0}\\ \mathbf{0} & \mathbf{0} & \cdots & \mathbf{0} & \mathbf{A}_N\end{bmatrix}, \quad (9)$$

and analogously for the memory function matrix $\boldsymbol{\Gamma}$, where $\mathbf{T}$ is a $nN\times nN$ block matrix defined as

$$\mathbf{T}=\begin{bmatrix}\beta_1\mathbf{1} & \beta_2\mathbf{1} & \beta_3\mathbf{1} & \cdots & \beta_{n-1}\mathbf{1} & 1/\sqrt{n}\mathbf{1}\\ -\beta_1\mathbf{1} & \beta_2\mathbf{1} & \beta_3\mathbf{1} & \cdots & \beta_{n-1}\mathbf{1} & 1/\sqrt{n}\mathbf{1}\\ \mathbf{0} & -2\beta_2\mathbf{1} & \beta_3\mathbf{1} & \cdots & \beta_{n-1}\mathbf{1} & 1/\sqrt{n}\mathbf{1}\\ \cdots & \cdots & \cdots & \cdots & \cdots & \cdots\\ \mathbf{0} & \mathbf{0} & \cdots & -(n-2)\beta_{n-2}\mathbf{1} & \beta_{n-1}\mathbf{1} & 1/\sqrt{n}\mathbf{1}\\ \mathbf{0} & \mathbf{0} & \mathbf{0} & \cdots & -(n-1)\beta_{n-1}\mathbf{1} & 1/\sqrt{n}\mathbf{1}\end{bmatrix}, \quad (10)$$

and $\beta_i=[i(i+1)]^{-1/2}$. By means of this transformation, the matrix $\mathbf{A}_{\text{tot}}$ is reduced to a block diagonal matrix with $n-1$ identical blocks on the diagonal,

$$\mathbf{A}_D=\frac{\beta l^2k_{\text{inter}}(t)}{3}[(n-1)\mathbf{1}+\mathbf{Q}_0\mathbf{Q}_0^T]+\mathbf{A}, \quad (11)$$

and one final block given by the matrix

$$\mathbf{A}_N=\frac{(n-1)\beta l^2k_{\text{inter}}(t)}{3}[\mathbf{1}-\mathbf{Q}_0\mathbf{Q}_0^T]+\mathbf{A}, \quad (12)$$

where the column vector $\mathbf{Q}_0$, whose transpose $\mathbf{Q}_0^T$

$=(N)^{-1/2}(1,...,1)$, is the Rouse eigenvector characterizing the center-of-mass coordinate. By this procedure, diagonalization of the $nN\times nN$ matrix $\mathbf{A}_{\mathrm{tot}}$ is reduced to the simple diagonalization of two $N\times N$ matrices $\mathbf{A}_D$ and $\mathbf{A}_N$.

By introducing the matrix $\mathbf{T}$, the generalized Langevin equation reduces to two main equations that are solved by diagonalization through the orthonormal eigenvector matrix $\mathbf{Q}$,

$$\mathbf{Q}=\mathbf{T}\begin{bmatrix}\mathbf{Q}_D & \mathbf{0} & \cdots & \mathbf{0}\\ \mathbf{0} & \mathbf{Q}_D & \cdots & \mathbf{0}\\ \cdots & \cdots & \cdots. & \cdots\\ \mathbf{0} & \mathbf{0} & \cdots & \mathbf{Q}_N\end{bmatrix}$$

$$=\begin{bmatrix}\frac{1}{\sqrt{2}}\mathbf{Q}_D & \frac{1}{\sqrt{6}}\mathbf{Q}_D & \cdots & \frac{1}{\sqrt{n(n-1)}}\mathbf{Q}_D & \frac{1}{\sqrt{n}}\mathbf{Q}_N\\ -\frac{1}{\sqrt{2}}\mathbf{Q}_D & \frac{1}{\sqrt{6}}\mathbf{Q}_D & \cdots & \frac{1}{\sqrt{n(n-1)}}\mathbf{Q}_D & \frac{1}{\sqrt{n}}\mathbf{Q}_N\\ \mathbf{0} & -\frac{2}{\sqrt{6}}\mathbf{Q}_D & \cdots & \frac{1}{\sqrt{n(n-1)}}\mathbf{Q}_D & \frac{1}{\sqrt{n}}\mathbf{Q}_N\\ \mathbf{0} & \mathbf{0} & \cdots & -\frac{n-1}{\sqrt{n(n-1)}}\mathbf{Q}_D & \frac{1}{\sqrt{n}}\mathbf{Q}_N\end{bmatrix}. \tag{13}$$

For each of the first $n-1$ blocks

$$\zeta_0\frac{d\mathbf{r}_D(t)}{dt}=-k_s\mathbf{A}_D\mathbf{r}_D(t)-\int_0^t\mathbf{\Gamma}_D(t-\tau)\frac{d\mathbf{r}_D(\tau)}{d\tau}d\tau+\mathbf{F}_D(t), \tag{14}$$

and for the final block

$$\zeta_0\frac{d\mathbf{r}_N(t)}{dt}=-k_s\mathbf{A}_N\mathbf{r}_N(t)-\int_0^t\mathbf{\Gamma}_N(t-\tau)\frac{d\mathbf{r}_N(\tau)}{d\tau}d\tau+\mathbf{F}_N(t), \tag{15}$$

where $\mathbf{\Gamma}_D=\mathbf{\Gamma}-\mathbf{\Gamma}'$ and $\mathbf{\Gamma}_N=\mathbf{\Gamma}+(n-1)\mathbf{\Gamma}'$. Moreover, we have that

$$\begin{bmatrix}\mathbf{r}_D\\ \mathbf{r}_D\\ \cdot\cdot\\ \mathbf{r}_D\end{bmatrix}=\begin{bmatrix}(2)^{-1/2}[\mathbf{r}^{(1)}-\mathbf{r}^{(2)}]\\ (6)^{-1/2}[\mathbf{r}^{(1)}+\mathbf{r}^{(2)}-2\mathbf{r}^{(3)}]\\ \cdots\cdots\cdots\cdots\\ [n(n-1)]^{-1/2}[\Sigma_{i=1}^{n-1}\mathbf{r}^{(i)}-(n-1)\mathbf{r}^{(n)}]\end{bmatrix}, \tag{16}$$

and

$$\mathbf{r}_N=\left[(n)^{-1/2}\sum_{i=1}^{n}\mathbf{r}^{(i)}\right]. \tag{17}$$

In normal-mode coordinates

$$\zeta_0\frac{d\mathbf{x}_D(t)}{dt}=-k_s\lambda_D\mathbf{x}_D(t)-\int_0^t\mathbf{Q}_D^{-1}\mathbf{\Gamma}_D(t-\tau)\mathbf{Q}_D\times\frac{d\mathbf{x}_D(\tau)}{d\tau}d\tau+\mathbf{F}_D'(t), \tag{18}$$

and

$$\zeta_0\frac{d\mathbf{x}_N(t)}{dt}=-k_s\lambda_N\mathbf{x}_N(t)-\int_0^t\mathbf{Q}_N^{-1}\mathbf{\Gamma}_N(t-\tau)\times\mathbf{Q}_N\frac{d\mathbf{x}_N(\tau)}{d\tau}d\tau+\mathbf{F}_N'(t), \tag{19}$$

where the eigenvalues λ_D are $n-1$ degenerate, the eigenvalues λ_N are nondegenerate, $\mathbf{F}_D'(t)=\mathbf{Q}_D^{-1}\mathbf{F}_D(t)$, and $\mathbf{F}_N'(t)=\mathbf{Q}_N^{-1}\mathbf{F}_N(t)$. Mode coordinates for the first $n-1$ equivalent blocks are defined as $\mathbf{x}_D=\mathbf{Q}_D^{-1}\mathbf{r}_D$, while mode coordinates for the final block are given by $\mathbf{x}_N=\mathbf{Q}_N^{-1}\mathbf{r}_N$.

The matrices of degenerate and nondegenerate eigenvalues are defined respectively as

$$\lambda_D=\frac{(n-1)\beta l^2k_{\mathrm{inter}}(t)}{3}\mathbf{1}+\lambda+\frac{\beta l^2k_{\mathrm{inter}}(t)}{3}\mathbf{Q}_D^{-1}\mathbf{Q}_0\mathbf{Q}_0^T\mathbf{Q}_D, \tag{20}$$

$$\lambda_N=\frac{(n-1)\beta l^2k_{\mathrm{inter}}(t)}{3}\mathbf{1}+\lambda-\frac{(n-1)\beta l^2k_{\mathrm{inter}}(t)}{3}\mathbf{Q}_D^{-1}\mathbf{Q}_0\mathbf{Q}_0^T\mathbf{Q}_D, \tag{21}$$

where λ are the eigenvalues of the intramolecular matrix $\mathbf{A}$. Since the center-of-mass diffusion in the Rouse model is decoupled from the other modes of motion, the last term in both equations is null except for the zero-order mode.

By means of the block diagonalization procedure described above, the problem reduces to the solution of nonlinear differential equations

$$\zeta_0\frac{d[\mathbf{x}_D(t)]_0}{dt}=-nG_{\mathrm{c.m.}}(t)[\mathbf{x}_D(t)]_0-\int d\tau[\Gamma(t-\tau)-\Gamma'(t-\tau)]_0\times\frac{d[\mathbf{x}_D(\tau)]_0}{d\tau}+[\mathbf{F}_D(t)]_0,$$

$$\zeta_0\frac{d[\mathbf{x}_D(t)]_p}{dt}=-[k_s\lambda_p+(n-1)G(t)][\mathbf{x}_D(t)]_p-\int d\tau[\Gamma(t-\tau)-\Gamma'(t-\tau)]_p\times\frac{d[\mathbf{x}_D(\tau)]_p}{d\tau}+[\mathbf{F}_D(t)]_p, \tag{22}$$

$$\zeta_0\frac{d[\mathbf{x}_N(t)]_0}{dt}=-\int d\tau[\Gamma(t-\tau)+(n-1)\Gamma'(t-\tau)]_0\times\frac{d[\mathbf{x}_N(\tau)]_0}{d\tau}+[\mathbf{F}_N(t)]_0,$$

and

$$\zeta_0\frac{d[\mathbf{x}_N(t)]_p}{dt}=-[k_s\lambda_p+(n-1)G(t)][\mathbf{x}_N(t)]_p - \int d\tau[\Gamma(t-\tau)+(n-1)\Gamma'(t-\tau)]_p \times\frac{d[\mathbf{x}_N(\tau)]_p}{d\tau}+[\mathbf{F}_N(t)]_p. \quad (23)$$

$G_{\text{c.m.}}(t)$ and $G(t)$ are the center-of-mass and monomer intermolecular time-dependent force strengths obtained, respectively, from the potentials in Eqs. (2) and (3). The inclusion of intermolecular forces in the dynamics of a group of chains moving cooperatively preserves the decoupling of center-of-mass and internal dynamics characteristic of the Rouse model (see the Appendix). Physically, this implies that the internal dynamics of a polymer does not depend on the choice of the reference system.

Memory contributions are given by $\Gamma_p=[\mathbf{Q}^{-1}\boldsymbol{\Gamma}\mathbf{Q}]_{p,p}$ and $\Gamma'_p=[\mathbf{Q}^{-1}\boldsymbol{\Gamma}'\mathbf{Q}]_{p,p}$, where the eigenvectors are not also necessarily eigenvectors of the memory function matrices. Time and space correlations of random forces obey the fluctuation-dissipation conditions

$$\langle[\mathbf{F}_D(t)]_p\cdot[\mathbf{F}_D(0)]_q\rangle=6\zeta_D\beta^{-1}\delta(t)\delta_{pq}, \quad (24)$$

$$\langle[\mathbf{F}_N(t)]_p\cdot[\mathbf{F}_N(0)]_q\rangle=6\zeta_N\beta^{-1}\delta(t)\delta_{pq}, \quad (25)$$

$$\langle[\mathbf{F}_D(t)]_p\cdot[\mathbf{F}_N(0)]_q\rangle=0, \quad (26)$$

where

$$\zeta_D=\zeta_0+\frac{\beta}{3}\sum_p\int_0^\infty d\tau[\Gamma_p(t-\tau)-\Gamma'_p(t-\tau)] \quad (27)$$

and

$$\zeta_N=\zeta_0+\frac{\beta}{3}\sum_p\int_0^\infty d\tau[\Gamma_p(t-\tau)+(n-1)\Gamma'_p(t-\tau)]. \quad (28)$$

IV. MODE-DEPENDENT DYNAMICS

In the following treatment (Secs. IV, V, and VI), we neglect contributions from the memory functions. This approximation holds when the linearized part of the Langevin equation is obtained from the projection of the fluid dynamics onto an extended set of relevant variables.[14] In the limiting case where all the relevant variables are taken into account in the projection operator, the memory contributions become negligible. We argue that this is the case in our approach, since we use an extended set of both intra- and intermolecular coordinates.

In addition, when only the intramolecular polymer coordinates are chosen as slow variables and the memory function is discarded, this procedure recovers the traditional Rouse equation that is a good zero-order description of the dynamics of short, unentangled polymer melts.

Normal-mode coordinates for the single-chain center-of-mass diffusion ($p=0$) are calculated as

$$[\mathbf{x}_D(t)]_0=[\mathbf{x}_D(0)]_0e^{-\alpha_0(t)} + e^{-\alpha_0(t)}\int_0^t d\tau\zeta_D^{-1}[\mathbf{F}_D(\tau)]_0e^{\alpha_0(\tau)} \quad (29)$$

and

$$[\mathbf{x}_N(t)]_0=[\mathbf{x}_N(0)]_0+\int_0^t d\tau\zeta_N^{-1}[\mathbf{F}_N(\tau)]_0, \quad (30)$$

where

$$\alpha_0(t)=\frac{n}{\zeta_D}\int_0^t G_{\text{c.m.}}(t')dt'. \quad (31)$$

Solutions of Eqs. (22) and (23) for the local dynamics ($p=1,...,N-1$) are given respectively by the equations

$$[\mathbf{x}_D(t)]_p=[\mathbf{x}_D(0)]_pe^{-t/(\tau_D)_p} + e^{-t/(\tau_D)_p}\int_0^t d\tau\zeta_0^{-1}[\mathbf{F}_D(\tau)]_pe^{\tau/(\tau_D)_p} \quad (32)$$

and

$$[\mathbf{x}_N(t)]_p=[\mathbf{x}_N(0)]_pe^{-t/(\tau_N)_p} + e^{-t/(\tau_N)_p}\int_0^t d\tau\zeta_0^{-1}[\mathbf{F}_N(\tau)]_pe^{\tau/(\tau_N)_p}, \quad (33)$$

where the characteristic relaxation times are defined as

$$\frac{t}{(\tau_D)_p}=\frac{k_s(\lambda_D)_pt}{\zeta_D}+\alpha(t) \quad (34)$$

and

$$\frac{t}{(\tau_N)_p}=\frac{k_s(\lambda_N)_pt}{\zeta_N}+\alpha(t), \quad (35)$$

where

$$\alpha(t)=\frac{n}{\zeta_D}\int_0^t G(t')dt'. \quad (36)$$

V. MEAN-SQUARE DISTANCES

The single-chain center-of-mass mean-square displacement is given by

$$\Delta R^2(t)=\langle[\mathbf{R}_{\text{c.m.}}(t)-\mathbf{R}_{\text{c.m.}}(0)]^2\rangle =N^{-2}\sum_{i,j=1}^N\left[\frac{n-1}{n}\sum_{p=0}^{N-1}(\mathbf{Q}_D)_{i,p}(\mathbf{Q}_D)_{j,p} \times\langle([\mathbf{x}_D(t)]_p-[\mathbf{x}_D(0)]_p)^2\rangle + \frac{1}{n}\sum_{p=0}^{N-1}(\mathbf{Q}_N)_{i,p}(\mathbf{Q}_N)_{j,p}\langle([\mathbf{x}_N(t)]_p-[\mathbf{x}_N(0)]_p)^2\rangle\right], \quad (37)$$

where we have made use of the property that $\Sigma_{i=1}^{n-1}[i(i+1)]^{-1}=(n-1)/n$. When the sum over segments is performed, Eq. (37) reduces to

$$\Delta R^2(t)=\frac{n-1}{nN}\langle\{[\mathbf{x}_D(t)]_0-[\mathbf{x}_D(0)]_0\}^2\rangle + \frac{1}{nN}\langle\{[\mathbf{x}_N(t)]_0-[\mathbf{x}_N(0)]_0\}^2\rangle. \quad (38)$$

From Eqs. (29) and (30), the effective single-chain diffusion coefficient is given by the contributions of relative and collective diffusion,

$$D=\frac{(n-1)}{6Nn}\frac{\partial\langle\{[\mathbf{x}_D(t)]_0-[\mathbf{x}_D(0)]_0\}^2\rangle}{\partial t}+\frac{1}{nN\beta\zeta_N}, \quad (39)$$

where

$$\langle\{[\mathbf{x}_D(t)]_0-[\mathbf{x}_D(0)]_0\}^2\rangle=\langle[\mathbf{x}_D(0)]_0^2\rangle(e^{-\alpha_0(t)}-1)^2 + \frac{6}{\beta\zeta_D}e^{-2\alpha_0(t)}\int_0^t e^{2\alpha_0(t')}dt'. \quad (40)$$

At long time intervals, if the polymer intermolecular potential is strong and attractive,[15] the relative diffusion is supressed and only collective dynamics take place: $\Delta R(t)^2=6D_ct$, with $D_c=D_{\text{Rouse}}/(\rho\sqrt{N})$. On the other hand, if the intermolecular interaction vanishes,

$$\Delta R(t)^2=\frac{6t}{\beta nN}\left(\frac{1}{\zeta_N}+\frac{(n-1)}{\zeta_D}\right), \quad (41)$$

which recovers the single chain dynamics when $\zeta_N=\zeta_D$.

The statistically averaged distance between the centers of mass of two different polymers at fixed time t is given in mode coordinates by

$$\langle[\mathbf{R}_{\text{c.m.}}^{(1)}(t)-\mathbf{R}_{\text{c.m.}}^{(2)}(t)]^2\rangle = N^{-2}\sum_{i,j=1}^{N}\left[\frac{n-1}{n}\sum_{p=0}^{N-1}\left[(\mathbf{Q}_D)_{i,p}^2+(\mathbf{Q}_D)_{j,p}^2 + \frac{2}{n-1}(\mathbf{Q}_D)_{i,p}(\mathbf{Q}_D)_{j,p}\right]\langle[\mathbf{x}_D(t)]_p^2\rangle + \frac{1}{n}\sum_{p=0}^{N-1}[(\mathbf{Q}_N)_{i,p}-(\mathbf{Q}_N)_{j,p}]^2\langle[\mathbf{x}_N(t)]_p^2\rangle\right] \quad (42)$$

$$=\frac{2}{N}\langle[\mathbf{x}_D(t)]_0^2\rangle, \quad (43)$$

where we used the definition of the diffusive normal mode, namely

$$N^{-1}\sum_{i=1}^{N}\sum_{p=0}^{N-1}(\mathbf{Q}_D)_{i,p}^2\langle[\mathbf{x}_D(t)]_p^2\rangle=(\mathbf{Q}_D)_0^2\langle[\mathbf{x}_D(t)]_0^2\rangle = N^{-1}\langle[\mathbf{x}_D(t)]_0^2\rangle \quad (44)$$

and analogously for the coordinates of nondegenerate modes.

The time-dependent relative distance between centers of mass of two polymers is

$$\langle[\mathbf{R}_{\text{c.m.}}^{(1)}(t)-\mathbf{R}_{\text{c.m.}}^{(2)}(t')]^2\rangle = \frac{n-1}{nN}\left[\langle[\mathbf{x}_D(t)]_0^2\rangle+\langle[\mathbf{x}_D(t')]_0^2\rangle + \frac{2}{n-1}\langle\mathbf{x}_D(t)_0\mathbf{x}_D(t')_0\rangle\right]+\frac{1}{nN}[\langle[\mathbf{x}_N(t)]_0\rangle - \langle[\mathbf{x}_N(t')]_0\rangle]^2. \quad (45)$$

When the position of two interacting polymers is sampled at a distance larger than the range of the intermolecular potential, or when sampling a time interval larger than the relaxation time scale for the intermolecular interaction,[10] the dynamics of the two chains becomes uncorrelated, so that

$$\langle[\mathbf{R}_{\text{c.m.}}^{(1)}(t)-\mathbf{R}_{\text{c.m.}}^{(2)}(t')]^2\rangle=\frac{1}{N}\langle[\mathbf{x}_N(t)]_0^2\rangle+\frac{1}{N}\langle[\mathbf{x}_N(t')]_0^2\rangle = \langle[\mathbf{R}_{\text{c.m.}}^{(1)}(t)-\mathbf{R}_{\text{c.m.}}^{(1)}(0)]^2\rangle + \langle[\mathbf{R}_{\text{c.m.}}^{(2)}(t')-\mathbf{R}_{\text{c.m.}}^{(2)}(0)]^2\rangle. \quad (46)$$

The time-dependent mean-square distance between two generic monomers i and j, belonging to the same polymer, is calculated from the equation

$$\langle[\mathbf{r}_i(t)-\mathbf{r}_j(0)]^2\rangle = \frac{n-1}{n}\sum_{p=0}^{N-1}\langle\{(\mathbf{Q}_D)_{i,p}[\mathbf{x}_D(t)]_p-(\mathbf{Q}_D)_{j,p}[\mathbf{x}_D(0)]_p\}^2\rangle + \frac{1}{n}\sum_{p=0}^{N-1}\langle\{(\mathbf{Q}_N)_{i,p}[\mathbf{x}_N(t)]_p-(\mathbf{Q}_N)_{j,p}[\mathbf{x}_N(0)]_p\}^2\rangle. \quad (47)$$

For weakly interacting polymers, the long-time, global-scale, many-chain dynamics becomes uncoupled, so that $\mathbf{Q}_N=\mathbf{Q}_D=\mathbf{Q}$, $\mathbf{x}_N\approx\mathbf{x}_D\approx\mathbf{x}$, and the conventional equation for single-chain dynamics is recovered:

$$\langle[\mathbf{r}_i(t)-\mathbf{r}_j(0)]^2\rangle=\sum_{p=0}^{N-1}\langle\{(\mathbf{Q})_{i,p}[\mathbf{x}(t)]_p-(\mathbf{Q})_{j,p}[\mathbf{x}(0)]_p\}^2\rangle, \quad (48)$$

where $\mathbf{Q}$ and $\mathbf{x}$ are, respectively, the eigenvectors and mode coordinates of the single-chain generalized Langevin equation.

The mean-square distance between two monomers i and j, belonging to two different chains k and l, is determined from the expression

$$\langle[\mathbf{r}_i^k(t)-\mathbf{r}_j^l(t')]^2\rangle = \frac{n-1}{n}\sum_{p=0}^{N-1}\left\{[(\mathbf{Q}_D)_{i,p}]^2\langle\{[\mathbf{x}_D(t)]_p\}^2\rangle + [(\mathbf{Q}_D)_{j,p}]^2\langle\{[\mathbf{x}_D(t')]_p\}^2\rangle + \frac{2}{n-1}(\mathbf{Q}_D)_{i,p}(\mathbf{Q}_D)_{j,p}\langle\{[\mathbf{x}_D(t)]_p\}\cdot\{[\mathbf{x}_D(t')]_p\}\rangle\right\} + \frac{1}{n}\sum_{p=0}^{N-1}\langle\{(\mathbf{Q}_N)_{i,p}[\mathbf{x}_N(t)]_p-(\mathbf{Q}_N)_{j,p}[\mathbf{x}_N(0)]_p\}^2\rangle. \quad (49)$$

In the long-time limit and/or at large distances, the dynamics of two interacting polymers becomes uncoupled, so that the monomer dynamics follows the equation

$$\langle[\mathbf{r}_i^k(t)-\mathbf{r}_j^l(t')]^2\rangle=\sum_{p=0}^{N-1}(\mathbf{Q})_{i,p}^2\langle[\mathbf{x}(t)]_p^2\rangle + \sum_{p=0}^{N-1}(\mathbf{Q})_{j,p}^2\langle[\mathbf{x}(t')]_p^2\rangle, \quad (50)$$

recovering the traditional "picture" of two polymer chains moving independently.[1]

VI. INTERPLAY BETWEEN SEMIFLEXIBILITY AND INTERMOLECULAR INTERACTIONS IN THE SINGLE-CHAIN DYNAMICS: MODEL CALCULATIONS

In this section, we investigate the effect of the interplay between intramolecular and intermolecular forces on the dynamics of an unentagled semiflexible polymer chain in a melt. We focus on polyethylene as a model system because of its technologically important applications and the abundance of available computational data.[2,8,9,19–21]

In our model calculations, each polymer chain is comprised of $N=100$ beads. We vary the intermolecular contributions at full interpolymer overlap $G_{\text{c.m.}}(0)$, and the local polymer semiflexibility calculated as a freely rotating chain with stiffness parameter g ($g=\langle\mathbf{l}_i\cdot\mathbf{l}_{i+1}\rangle/l^2$). For polyethylene (PE) chains $g=0.74$. In general, the monomer $G(0)\approx 0$ at any relevant intermolecular space scale, so we simply neglect it.

We use for the effective monomer friction coefficient, temperature, and density the values reported in the literature for a system widely investigated,[2,8,19] with $\zeta_{\text{eff}}=0.2\times10^{-9}$ dyn s/cm, $T=509$ K, and $\rho=0.733$ g/cm^3. The initial average interpolymer distance $R^2(0)$ is determined by the density of the system and the pair distribution function through the space-dependent center-of-mass distribution $n(r)$ as

$$R^2(0)\approx\int_0^{\sim R_g} n(r)r^2dr \Big/ \int_0^{\sim R_g} n(r)dr,$$

$$n(r)=N^{-1}\int_0^r d\mathbf{r}'\rho g(\mathbf{r}'). \quad (51)$$

Different $R^2(0)$ values only slightly affect the dynamics in the very short-time regime, while the qualitative behavior does not change.

A. Normal modes of motion

Single-chain dynamics deviates from Rouse behavior due to semiflexibility and dynamical correlation. As a starting point, we focus on the static correlation of modes as a function of polymer stiffness. In Fig. 1, we plot $\langle\mathbf{x}_p(0)^2\rangle=l^2/\lambda_p$ as a function of p^{-2} with increasing polymer stiffness, normalized by its rod value. For continuous ($N\to\infty$), totally flexible ($g=0$), single-chain [$G(t)=0$] dynamics, the Rouse model predicts that the static correlation of modes follows $\langle\mathbf{x}_p(0)^2\rangle\approx(N-1)^2l^2/(6\pi^2p^2)$ with $p\geqslant1$. In the opposite limit of a completely stiff polymer, the only possible modes of motion are translation ($p=0$) and rotation ($p=1$). However, $(\lambda_0)_{\text{rod}}=0$ and $(\lambda_1)_{\text{rod}}=12(N-1)^{-3}$, which gives $\langle\mathbf{x}_1(0)^2\rangle_{\text{rod}}=l^2(N-1)^3/12$. By increasing polymer stiffness ($g\to1$), the first eigenvalue approaches $(\lambda_1)_{\text{rod}}$ asymptotically while the other eigenvalues tend to zero.

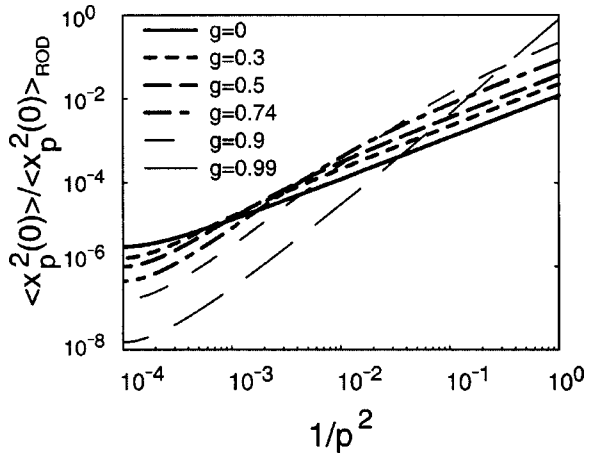

FIG. 1. Static correlation of the intramolecular normal modes at increasing stiffness parameter g, as a function of the inverse square mode index p. The function is normalized by its value for a rod polymer.

A plot of the normalized $\langle\mathbf{x}_p(0)^2\rangle$ shows some interesting features (Fig. 1). By increasing the local stiffness in a chain with a fixed number of statistical segments $N-1$, the overall dimension of the polymer increases [$\langle\mathbf{x}_1(0)^2\rangle_{\text{flex}}\propto(N-1)^2$ while $\langle\mathbf{x}_1(0)^2\rangle_{\text{rod}}\propto(N-1)^3$]. An increase in the local polymer stiffness also modifies the scaling with the mode index of $\langle\mathbf{x}_p(0)^2\rangle$. For flexible polymers, the scaling follows Rouse as $\langle\mathbf{x}_p(0)^2\rangle\propto p^{-2}$, while by increasing g, higher-index modes appear to follow $\langle\mathbf{x}_p(0)^2\rangle\propto p^{-3}$. For polyethylene melts ($g=0.74$), calculation of the normalized square amplitude of modes for $N=100$ is shown in Fig. 2, where every seventh mode is reported: the calculated global dynamics follows the p^{-2} scaling while the dynamics at an intermediate scale follows p^{-3}. This effect was originally found in computer simulations of PE melts (see Fig. 10 in

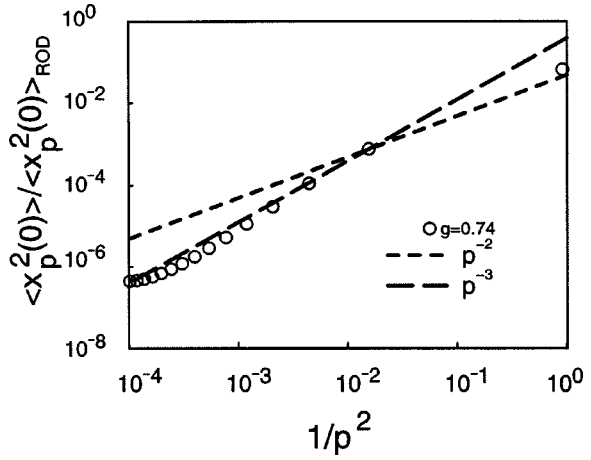

FIG. 2. Normalized static correlation of the intramolecular normal modes as a function of the inverse square mode index p, for a polyethylene chain, reported every seventh mode. Also shown are the p^{-2} and p^{-3} scaling functions.

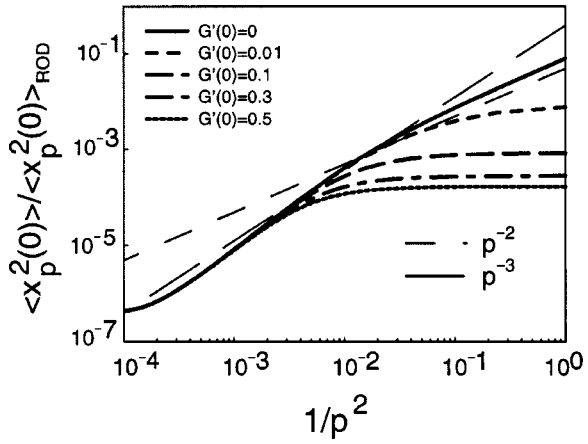

FIG. 3. Normalized static correlation of intramolecular normal modes as a function of the inverse square mode index p, at increasing strength of the intermolecular force. The p^{-2} and p^{-3} scaling functions are also shown.

Ref. 8) and, although a physical explanation of this phenomenon was not presented, this feature was the basis of an empirical equation proposed by Ediger to explain recent experiments of the time correlation function $P_2(t)$ for PE melt dynamics.[9] From our calculations, this feature emerges as a characteristic of local polymer stiffness. We suggest that the p^{-3} scaling is consistent with the fact that polyethylene chains are stiff at scales smaller than their persistence length, while at larger distances the polymer can be described as a flexible chain of renormalized segments following a p^{-2} scaling. On the length scale of the statistical persistence length, which for PE is about $N'=10$,[19] the polymer behaves like a rod and $\langle \mathbf{x}_p^2(0)\rangle \propto l^2 N'^3$; while at a length scale of the local bond distance $\langle \mathbf{x}_{N'}^2(0)\rangle \propto l^2 (N')^0$. The scaling with p for modes acting on length scales smaller than the statistical segment must obey $\langle \mathbf{x}_p^2(0)\rangle \propto l^2 N'^3 p^{-3}$ to recover the correct limits at the persistence length and at the local bond length.

In Fig. 3, we analyze the effect of the intermolecular force on the static correlation of modes for a semiflexible ($g=0.74$) polymer. By increasing the intensity of the intermolecular interaction at time zero, $G(0)=0$, 0.01, 0.1, 0.3, 0.5, we observe that the presence of intermolecular forces perturb modes starting from a large scale, while local modes are not affected. Only at high intermolecular forces are modes on the local scale finally perturbed. In the region where intermolecular effects are dominant, the static correlation of modes is independent of mode index. This suggests that molecular relaxation, when strong intermolecular forces are present, is driven on a large scale by intermolecular interactions with global intramolecular modes frozen, while on a local spatial scale the intramolecular modes are still active. This effect is in qualitative agreement with data from experiments and computer simulations for systems with high intermolecular interactions.[20,22] The modes of motion are orthogonal, in agreement with data from computer simulations of unentangled semiflexible polymer melts,[8] entangled polymer melts, and undercooled unentangled polymer melts,[22] which indicates that the onset of anomalous dynamics is not a consequence of correlation between mode pairs.

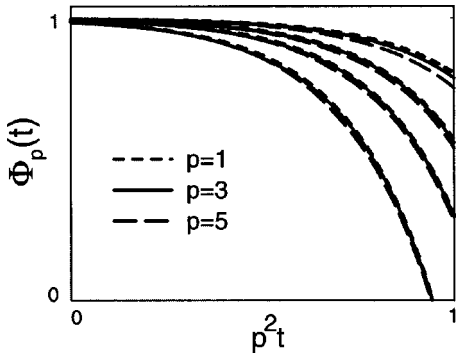

FIG. 4. Time-dependent correlation of the intramolecular normal modes as a function of the product of the square normal mode index p and time, with increasing polymer stiffness (from top to bottom, $g=0.74$, 0.5, 0.3, and 0).

The time-dependent correlation of relaxation modes, $\Phi_p(t)=\langle \mathbf{x}_p(t)\cdot \mathbf{x}_p(0)\rangle / \langle \mathbf{x}_p^2(0)\rangle$, presents an analogous behavior. In the continuous Rouse model ($N\to\infty$),[1] $\Phi_p(t)$ decays as a simple exponential function $\Phi_p(t) \propto \exp[-p^2 t/(\tau_{\text{Rouse}})]$. By plotting $\Phi_p(t)$ as a function of $p^2 t$, it is possible to emphasize the anomalies in the mode decay with respect to the Rouse model, for which all modes follow a universal relaxation curve. In Fig. 4, we show the decay of $\Phi_p(t)$ for modes $p=1$, 3, and 5 for a finite Gaussian chain of increasing stiffness, $g=0$, 0.3, 0.5, and 0.74. For $g=0$, the fastest decay, curves for different modes superimpose almost exactly, with a slight discrepancy due to the finite size of the chain. However, when the internal rigidity increases, the decay of different modes starts to separate, with higher-order modes (local dynamics) relaxing much faster than the first mode (global dynamics): in the rod limit, the only mode of relaxation is rotation ($p=1$), while $\lambda_p \to 0$ ($\tau_p \to \infty$) for $p\neq 1$.

In Fig. 5, we analyze the mode decay as a function of increasing intermolecular interaction $G(0)=0$, 0.01, 0.1, 0.3, and 0.5 for modes $p=1$, 3, and 5. The effect of an in-

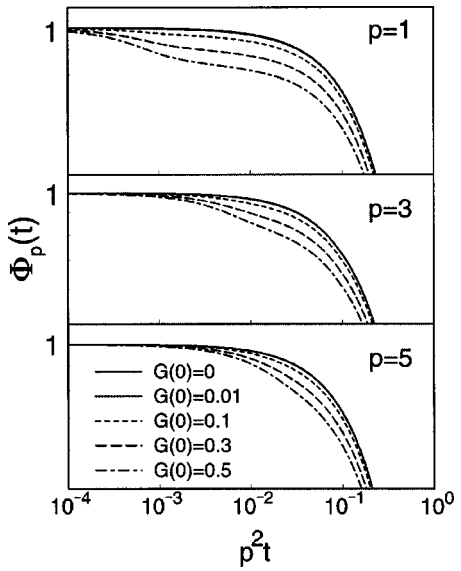

FIG. 5. Time-dependent correlation of intramolecular normal modes as a function of the product of the square normal mode index p and time, for the first three modes, with increasing strength of the intermolecular force.

crease in $G(0)$ is quite relevant on short time scales ($t \leqslant \tau_{\text{Rouse}}$), where the dynamics shows the formation of a plateau and the decay becomes a double exponential. The presence of intermolecular interactions affects the decay of normal modes with a most dramatic effect seen for modes of low index (global dynamics) p. Intermolecular forces mainly perturb the dynamics on the global spatial scale, while the local dynamics remains unperturbed. This effect agrees with the experimental observation of the mode decay in systems with increasing strength of intermolecular interactions.[20,22]

For unentangled PE melt dynamics, we predict that the decay of normal modes is affected by the presence of chain semiflexibility, which induces deviations from the p^2t scaling mainly on the local scale (high-index modes), and by the intermolecular forces which induce a faster decay of the short-time global dynamics (low-index modes). As a result, a complex path of mode relaxation appears for this system.[2,8]

B. Mean-square displacements

Experimental data and computer simulations of monomer mean-square displacements for PE unentangled melt dynamics are in overall agreement with Rouse dynamics, save the intermediate regime where a scaling in time stronger than the Rouse $t^{0.5}$ is observed.[4,19] Rouse theory predicts for the monomer mean-square displacement at short time scales to be

$$\Delta\mathbf{r}^2(t)=\langle[\mathbf{r}_{N/2}(t)-\mathbf{r}_{N/2}(0)]^2\rangle=6Dt(N+1), \tag{52}$$

while for longer times, but still smaller than the longest Rouse relaxation time, the monomer mean-square displacement follows anomalous dynamics [$\Delta\mathbf{r}^2(t)\propto t^{0.5}$]

$$\Delta\mathbf{r}^2(t)=\sqrt{\frac{12Nl^2Dt}{\pi}}. \tag{53}$$

Only at $t\approx\tau_{\text{Rouse}}$ does $\Delta\mathbf{r}^2(t)$ cross over to the center-of-mass Fickian dynamics [$\Delta\mathbf{r}^2(t)\propto t$].

The observed disagreement between computer simulations and the Rouse approach is not surprising since the chain in the Rouse model follows the statistics of an infinite, freely jointed chain, i.e., a completely flexible polymer. Quite obviously, ''real'' macromolecules have local energy barriers and are of finite size. Reasonable agreement with the observed scaling exponent is obtained when we adopt a freely rotating chain description[26] of a finite-size molecule, with a stiffness parameter $g=0.74$, which is the value derived from the characteristic ratio of polyethylene.[15,16]

The effect of local energy barriers on polymer dynamics is most evident on the local, monomeric scale. In fact, once the finite size of the molecule is included in the calculation, the freely jointed model (no local stiffness) is equivalent to the more realistic freely rotating chain model (with local stiffness) only for properties on length scales larger than the local persistence length. The freely jointed chain with effective statistical bonds works well on a global spatial scale, but describes very poorly the properties at the monomer scale.

On the other hand, finite-size effects will affect dynamics mostly on the global, center-of-mass scale. Unless the polymer is quite short (on the order of the local persistence length), the dynamics of the central monomer is uncorrelated with the motion of end monomers, and it does not change when we consider polymer chains of increasing N. Evidently, when unentangled melt dynamics is under study, as is done here, chains can be quite short. In this case, both semiflexibility and finite-size effects play a role in the onset of anomalous dynamics and need to be properly taken into account.

In general, the monomer mean-square displacement appears to be independent of the presence of intermolecular forces. For example, from a mode analysis of local dynamics of unentangled polymer melts at the crossover to entangled dynamics (where intermolecular effects become more important), Richter and co-workers[20] showed that intermolecular forces affect the lower-index modes of motion. In this way, the dynamics is perturbed mainly on the global scale, while on the local scale it remains Rousian. Consistently, computer simulation results for the monomer mean-square displacement for entangled polymer melts appear to follow Rousian dynamics.[23,24]

On the whole, these data suggest that the mean force intermolecular potential affects monomer dynamics to a lesser extent than it does center-of-mass dynamics. This effect is consistent with the accepted ''physical picture'' of the polymer statistical configuration in the melt, where the polymer assumes an equilibrium unperturbed conformation because the intramolecular and intermolecular forces are equivalent in strength and compensate each other.[25] The monomer experiences a mean-field-like environment where it cannot distinguish between the intramolecular and intermolecular nature of forces.

Since the dynamical anomalies mainly affect the first mode of motion, the overall polymer dimension is only slightly affected by the presence of dynamically heterogeneous regions in the melt, and the polymer radius of gyration is nearly unperturbed, so that

$$R_g^2(t)=N^{-1}\sum_{p=1}^{N-1}\langle\mathbf{x}_p^2(t)\rangle\left[\sum_{i=1}^{N}\mathbf{Q}_{i,p}^2-N^{-1}\sum_{i,j=1}^{N}\mathbf{Q}_{i,p}\mathbf{Q}_{j,p}\right], \tag{54}$$

where $\langle\mathbf{x}_p^2(t)\rangle\approx\langle\mathbf{x}_p^2(0)\rangle$ is the square amplitude of mode p, and $\mathbf{Q}_{i,p}$ is the eigenvector for bead i of the matrix $\mathbf{A}_{\text{tot}}$. Notice that the first mode of motion does not appear in the calculation of the radius of gyration and that $R_g^2(t)$ is not affected by anomalies in the center-of-mass dynamics.

A complete analysis of the validity of our approach in predicting the center-of-mass anomalous diffusion has been extensively presented in previous papers.[15,16] Here, we briefly report our findings. Center-of-mass dynamics in computer simulations presents a short-time anomalous behavior characterized by an intermediate slowdown of the dynamics. The initial center-of-mass mean-square displacement follows a subdiffusive regime, $\nu=0.75-0.9$, which crosses over to the Rouse diffusion regime at $t\approx\tau_{\text{Rouse}}$. This effect, which is in disagreement with Rousian theory, has been qualitatively attributed to the presence of intermolecular forces. By means of our approach, we formally relate the strength and shape of the intermolecular potential to the appearance of anomalous diffusive behavior. Quite successfully, the theory quantita-

tively predicts the correct behavior upon best fitting the intermolecular potential at zero interpolymer distance with computer simulations.[15,16]

VII. CONCLUSIONS

In this paper, we present the theory for the dynamics of unentangled semiflexible polymers of finite size in a dynamically heterogeneous fluid. Because our approach explicitly includes local flexibility and the finite size of the polymer, it is possible to test its predictions versus experimental data and computer simulations.

The interplay between intermolecular interactions and internal polymer semiflexibility drives the onset of anomalous dynamics in polymer melts. The dynamical heterogeneity of the matrix, and its intermolecular interaction with the tagged chain, mainly affect global polymer dynamics by inducing a subdiffusive center-of-mass regime and a stretched relaxation of lowest modes in the time correlation function. Local dynamics, instead, strongly depend on polymer semiflexibility, which is a consequence of the local chemical structure. The presence of stiffness induces the p^{-3} anomalous scaling of the static correlation of modes at intermediate normal modes, observed experimentally in polyethylene melts. Global and local mean-square displacements from simulation data are quantitatively reproduced by this approach.

ACKNOWLEDGMENT

The author acknowledges support from the National Science Foundation under Grant No. DMR-0207949.

APPENDIX: HETEROGENEOUS DYNAMICS IN BOND VARIABLES

The single-chain center-of-mass dynamics is decoupled from polymer internal dynamics also when intermolecular forces are explicitly taken into account. This is conveniently shown when Eq. (4) is reformulated in bond variables. We make use of the beads-to-bonds transformation $\mathbf{l}(t)=\mathbf{M}\mathbf{r}(t)$, where $\mathbf{M}_{1,i}=N^{-1}$ for $i=1,...,N$, $\mathbf{M}_{i,i}=1$ for $i=2,...,N$, $\mathbf{M}_{i+1,i}=-1$ for $i=1,..., N-1$, and $\mathbf{M}_{i,j}=0$ otherwise. The static bond correlation matrix is $\mathbf{U}^{-1}_{i,j}=\langle \mathbf{l}_i\cdot\mathbf{l}_j\rangle/\mathbf{l}^2$, and contains information on the local semiflexibility. By introducing the transformation to bond variables, Eqs. (14) and (15) reduce to a set of $n-1$ coupled equations (for sake of simplicity we omit the memory function), namely

$$\zeta_0\frac{d\mathbf{l}_D(t)}{dt}=-\left[k_s\mathbf{M}\mathbf{M}^{\mathbf{T}}\begin{bmatrix}\mathbf{0} & \mathbf{0}\\ \mathbf{0} & \mathbf{U}\end{bmatrix}+(n-1)k_{\mathrm{inter}}(t)+\begin{bmatrix}\mathbf{1} & \mathbf{0}\\ \mathbf{0} & \mathbf{0}\end{bmatrix}k_{\mathrm{inter}}(t)\right]\mathbf{l}_D(t)+\mathbf{F}'_D(t), \tag{A1}$$

and

$$\zeta_0\frac{d\mathbf{l}_N(t)}{dt}=-\left[k_s\mathbf{M}\mathbf{M}^{\mathbf{T}}\begin{bmatrix}\mathbf{0} & \mathbf{0}\\ \mathbf{0} & \mathbf{U}\end{bmatrix}+(n-1)k_{\mathrm{inter}}(t)-\begin{bmatrix}\mathbf{1} & \mathbf{0}\\ \mathbf{0} & \mathbf{0}\end{bmatrix}(n-1)k_{\mathrm{inter}}(t)\right]\mathbf{l}_N(t)+\mathbf{F}'_N(t), \tag{A2}$$

where $\mathbf{F}'_D(t)=\mathbf{M}\mathbf{F}_D(t)$, $\mathbf{F}'_N(t)=\mathbf{M}\mathbf{F}_N(t)$, $\mathbf{l}_D=\mathbf{M}\mathbf{r}_D$, and $\mathbf{l}_N=\mathbf{M}\mathbf{r}_N$.

The matrix

$$\mathbf{M}\mathbf{M}^T=\begin{bmatrix}\frac{1}{N} & 0 & 0 & 0 & \cdots & 0\\ 0 & 2 & -1 & 0 & \cdots & 0\\ 0 & -1 & 2 & -1 & \cdots & 0\\ 0 & 0 & -1 & 2 & \cdots & 0\\ \cdots & \cdots & \cdots & \cdots & \cdots & \\ 0 & \cdots & 0 & 0 & -1 & 2\end{bmatrix}, \tag{A3}$$

has a block structure, where the element 1,1 refers to the center of mass. This bond-coordinate formulation of the dynamics shows clearly that there is no coupling between center-of-mass and internal dynamics, so it is possible to separate their equations of motion. Let us define the $(N-1)\times(N-1)$ matrix product

$$\mathbf{L}=\mathbf{a}\mathbf{a}^T\mathbf{U}, \tag{A4}$$

where $\mathbf{a}$ is the $(N-1)\times N$ matrix obtained from the matrix $\mathbf{M}$ when the first row is discarded. Center-of-mass dynamics is driven by two coupled equations,

$$\zeta_0\frac{d\mathbf{l}_{D,0}(t)}{dt}=-nk_{\mathrm{inter}}(t)\mathbf{l}_{D,0}(t)+\mathbf{F}'_{D,0}(t) \tag{A5}$$

and

$$\zeta_0\frac{d\mathbf{l}_{N,0}(t)}{dt}=\mathbf{F}'_{N,0}(t). \tag{A6}$$

Bond coordinates follow the equations of motion

$$\zeta_0\frac{d\mathbf{l}_D(t)}{dt}=-[k_s\mathbf{L}+(n-1)k_{\mathrm{inter}}(t)]\mathbf{l}_D(t)+\mathbf{F}'_D(t) \tag{A7}$$

and

$$\zeta_0\frac{d\mathbf{l}_N(t)}{dt}=-[k_s\mathbf{L}+(n-1)k_{\mathrm{inter}}(t)]\mathbf{l}_N(t)+\mathbf{F}'_N(t). \tag{A8}$$

The equations are solved through normal mode analysis and produce dynamical relations analogous to the ones derived for beads coordinates, discussed in Secs. III, IV, and V. The equations in bead coordinates can be formally recovered by applying the bonds-to-beads transformation to the equations in bond variables described here.

[1] M. Doi and S. F. Edwards, *The Theory of Polymer Dynamics* (Oxford University Press, Oxford, 1986).
[2] W. Paul, G. D. Smith, D. Y. Yoon, B. Frago, S. Rathgeber, A. Zirkel, L. Willner, and D. Richter, Phys. Rev. Lett. **80**, 2346 (1998).
[3] G. D. Smith, W. Paul, M. Monkenbush, and D. Richter, J. Chem. Phys. **114**, 4285 (2001).
[4] J. T. Padding and W. J. Briels, J. Chem. Phys. **114**, 8685 (2001).
[5] J. T. Padding and W. J. Briels, J. Chem. Phys. **115**, 2846 (2001).
[6] T. Kreer, J. Baschnagel, M. Muller, and K. Binder, Macromolecules **34**, 1105 (2001).
[7] L. Harnau, R. G. Winkler, and P. Reineker, Phys. Rev. Lett. **82**, 2408 (1999).
[8] W. Paul, G. D. Smith, and D. Y. Yoon, Macromolecules **30**, 7772 (1997).
[9] X. H. Qiu and M. D. Ediger, Macromolecules **33**, 490 (2000).
[10] M. G. Guenza, E. B. Webb, III, and G. S. Grest, Phys. Rev. Lett. (to be published).

[11] A. H. Marcus, J. Schofield, and S. A. Rice, Phys. Rev. E **60**, 5725 (1999).
[12] E. R. Weeks, J. C. Crocker, A. C. Levitt, A. Schofield, and D. A. Weitz, Science **287**, 627 (2000).
[13] M. Guenza, J. Chem. Phys. **110**, 7574 (1999).
[14] J. P. Hansen and I. R. McDonald, *Theory of Simple Liquids* (Academic, London, 1991).
[15] M. Guenza, Macromolecules **35**, 2714 (2002).
[16] M. Guenza, Phys. Rev. Lett. **88**, 025901 (2002).
[17] P. G. Bolhuis, A. A. Louis, and J. P. Hansen, J. Chem. Phys. **114**, 4296 (2001); A. A. Louis, P. G. Bolhuis, J. P. Hansen, and E. J. Maijer, Phys. Rev. Lett. **85**, 2522 (2000).
[18] A. Perico and M. Guenza, J. Chem. Phys. **83**, 3103 (1985); **84**, 510 (1986).
[19] W. Paul, D. Y. Yoon, and G. D. Smith, J. Chem. Phys. **103**, 1702 (1995).
[20] D. Richter, L. Willner, A. Zirkel, B. Frago, L. J. Fetters, and J. S. Huang, Phys. Rev. Lett. **71**, 4158 (1993).
[21] D. S. Pearson, L. J. Fetters, W. W. Graessley, G. Ver Strate, and E. von Meerwall, Macromolecules **27**, 711 (1994).
[22] K. Okun, M. Wolfgardt, J. Baschnagel, and K. Binder, Macromolecules **30**, 3075 (1997); C. Bennemann, W. Paul, K. Binder, and B. Dunweg, Phys. Rev. E **57**, 843 (1998).
[23] K. Kremer and G. S. Grest, J. Chem. Phys. **92**, 5057 (1990).
[24] A. Kolinski, J. Skolnick, and R. Yaris, J. Chem. Phys. **86**, 1567 (1987); S. W. Smith, C. K. Hall, and B. D. Freeman, *ibid.* **104**, 5616 (1996).
[25] P.-G. de Gennes, *Scaling Concepts in Polymer Physics* (Cornell University Press, Ithaca, NY, 1979).
[26] H. Yamakawa, *Modern Theory of Polymer Solutions* (Harper & Row, New York, 1971).